Discrete Stochastic Cascade Dynamics on Finite Graphs with Irreversible Energy Depletion

Part I: Construction, Guarantees, and Phase Structure

Shiv Goswami*

TERRAFLOCK PVT LTD, Bihar, India

ORCID 0009-0006-1554-9241 · shivgoswami.com

github.com/Shiv2071/Discrete-cascade-model

July 9, 2026

Abstract

We construct a new class of discrete stochastic dynamical systems on finite graphs that generate rich, transient structure from irreversible resource consumption alone. Two fundamentally asymmetric excitation species, distinguished by intrinsic frequency and self-interaction rules, interact stochastically while drawing from a strictly non-renewable local energy field; the cross-species interaction efficiency is modulated by the phase alignment of the two species, so that the frequency mismatch imprints a beat on the dynamics. Four coupled state variables (excitation counts, capacity energy, structural state, and a ripple measure) evolve through layered update rules that produce three dynamical regimes: quiescent, dissipative leakage, and explosive pair creation. A Landau-type free-energy functional governs bond formation, embedding a Landau-type order–disorder transition at the level of the local bond-formation rule, giving rise to a four-level structural hierarchy (excitation $\to$ pair $\to$ bond $\to$ clump).

We establish three rigorous guarantees. *Energy Monotonicity:* the total capacity energy is a non-negative supermartingale that decreases strictly in expectation whenever the system is active, providing a built-in thermodynamic arrow. *Finite Activity Bound:* the cumulative number of interactions across all space and time is almost surely finite, bounded by the ratio of initial energy to unit interaction cost. *Almost Sure Absorption:* the system reaches a frozen absorbing configuration in finite time with probability one, without requiring fine-tuning to a critical point.

Beyond these guarantees, we identify a transient complexity regime: we prove that structural diversity, initially zero, becomes strictly positive in the cascade regime and eventually freezes at a constant value, and we observe consistently in simulation that it passes through a peak (rising through explosive cascades, then

*Contact author: shiv@terraflock.com

decaying as energy is exhausted). We derive the principal regions of a phase diagram over initial energy density and interaction strength. The resulting framework demonstrates that spatial structure, self-amplifying cascades, metastable bonded configurations, and guaranteed finite-time termination can all emerge from purely discrete rules with no continuum limit, no external drive, and no infinite-resource assumption.

Keywords: interacting particle systems; absorbing-state phase transitions; stochastic cascades; irreversible dynamics; discrete dynamical systems; Landau phase transition

Contents

1 Introduction

1.1 Motivation

The standard mathematical description of motion rests on a chain of continuum assumptions: space is $\mathbb{R}^d$, time is $\mathbb{R}$, trajectories are smooth (or at least piecewise differentiable), and evolution is governed by differential equations whose solutions require limits over infinitely fine subdivision. This framework, formalised through calculus, has been extraordinarily successful. Yet it carries a foundational dependence on the completed infinite: every derivative is a limit, every integral an infinite sum, and every trajectory the result of infinitely many infinitesimal steps.

This dependence is not merely aesthetic. Zeno's dichotomy, that an object traversing a distance must first traverse half, then half the remainder, *ad infinitum*, is resolved in calculus by the convergence of geometric series, but the resolution presupposes exactly the continuum structure that the paradox questions. If one asks not "does the series converge?" but "can we build dynamics that do not *require* infinite subdivision?", a different programme emerges: replace smooth trajectories with discrete evolution rules, replace fields on $\mathbb{R}^d$ with states on finite graphs, and replace conservation laws with irreversible resource budgets.

The goal is not to refute calculus, whose empirical adequacy is beyond question, but to construct a self-contained dynamical framework in which:

(i) space is a finite graph with no notion of subdivision,

(ii) evolution proceeds in discrete steps with no limiting process,

(iii) two asymmetric excitation species interact stochastically,

(iv) a strictly non-renewable capacity energy imposes irreversibility, and

(v) threshold-driven regime switching generates qualitative diversity from quantitative variation.

The result is a minimal system that generates rich transient dynamics, including spatial structure, self-amplifying cascades, and metastable bonded configurations, yet is guaranteed to freeze into an absorbing state in finite time. Motion, geometry, and thermodynamic direction emerge from the interplay of discrete rules rather than from continuum assumptions.

1.2 Related Work

This work is related to interacting particle systems, reaction–diffusion models, and discrete stochastic dynamics [Pastor-Satorras et al., 2015, Mallick, 2015, Muñoz, 2018, Täuber, 2017]. However, it differs fundamentally in that it incorporates a finite, non-renewable energy constraint [Böttcher et al., 2015, Seifert, 2012], structural memory, and asymmetry-driven phase transitions, leading to provable absorption and bounded activity without requiring continuum limits [Bertini et al., 2015].

The model sits at the intersection of several classical threads. We discuss each, emphasising the precise structural features that distinguish the present system.

Interacting particle systems. The contact process [Harris, 1974, Liggett, 1999, Grimmett, 1999] and voter model study binary-state agents on lattices with local stochastic transitions [Van Kampen, 1992]. Multi-type extensions [Neuhauser, 1992, Durrett & Levin, 1994, Galla, 2011] introduce species diversity but retain infinite-time, stationary-measure analysis and impose symmetric or nearly-symmetric interaction kernels. Unlike multi-type contact processes, where species typically share the same interaction kernel or differ only in rates, our model imposes a *structurally forbidden* channel ($\alpha_{YY} = 0$) that makes the species non-interchangeable. Unlike classical IPS on infinite lattices, the system runs on a finite, non-renewable energy field that couples all transitions to a shared resource. The state space additionally includes a structural memory variable S that accumulates irreversibly, absent from classical IPS frameworks.

Absorbing-state phase transitions. Directed percolation universality [Hinrichsen, 2000, Henkel et al., 2008, Janssen, 1981] governs the transition from an active to an absorbing phase in many one-component systems, and comprehensive surveys [Marro & Dickman, 1999, Ódor, 2004, Täuber, 2014] catalogue the universality classes that arise under various symmetries and conservation laws. In those models the absorbing transition is a *phase boundary*: the system absorbs only when a control parameter is tuned below a critical value. Unlike directed percolation systems, where absorption requires tuning a control parameter below a critical value, our model guarantees absorption for *all* parameter values, because the driving resource is finite and strictly consumed.

Self-organised criticality. Sandpile models [Bak et al., 1987, Dhar, 1990, Chopard & Droz, 1998] exhibit power-law avalanche distributions through slow external driving balanced by fast relaxation (separation of timescales). Unlike sandpile models, our system has *no external drive*: it runs on a finite initial endowment. The transient complexity peak we identify (theorem 4.4) is analogous to the SOC steady state but is inherently non-stationary and terminal: it arises, persists while energy permits cascades, and vanishes as the resource is exhausted.

Reaction–diffusion systems. Continuous-space models of two-species annihilation ($A + B \to \varnothing$) and branching ($A \to 2A$) exhibit rich kinetics including anomalous density decay and segregation phenomena [Toussaint & Wilczek, 1983, Lee, 1994, Bramson & Lebowitz, 1988, Krapivsky et al., 2010, Peliti, 1985]. Unlike $A+B$ annihilation, where the density decays and nothing persists, our framework adds (i) energy budgets that bound total activity a.s., (ii) threshold-driven regime switching (quiescent $\to$ leakage $\to$ explosive), and (iii) a structural accumulation field that provides irreversible memory of past interactions. The system does not merely annihilate; it builds a frozen record of its interaction history [Berestycki et al., 2009].

Non-equilibrium Landau theory. Landau free-energy expansions are a standard tool in equilibrium phase transitions [Landau, 1937]. Their extension to driven and non-equilibrium systems [Hohenberg & Halperin, 1977, Cross & Hohenberg, 1993, Privman, 1997] typically assumes a stationary or slowly-varying background. Unlike non-equilibrium Landau models that assume a stationary or slowly-driven background, we import the Landau functional into a *transient*, far-from-equilibrium setting where the background (energy, excitation counts) is irreversibly depleted. The quasi-static

approximation is justified by timescale separation between fast local bond dynamics and slow global energy decay (theorem 2.15).

The gap this paper addresses. To our knowledge, existing frameworks do not simultaneously establish that a discrete, finite-resource stochastic system can produce a multi-level structural hierarchy (excitation → pair → bond → clump) with provably guaranteed termination. Specifically: contact processes and multi-type IPS lack structural memory and require parameter tuning for absorption; sandpile models require external driving; reaction–diffusion annihilation produces no persistent structure; and Landau theory has not been applied in a transient, irreversibly depleting context. The present model closes this gap by combining multi-species asymmetry, a finite energy resource, Landau bond formation, and regime switching into a single system with three rigorous guarantees. Table 1 in the Discussion provides a systematic comparison.

1.3 Contributions

This paper makes four contributions:

1. **A new dynamical system class.** We define a fully discrete, finite-resource stochastic system on arbitrary finite graphs, coupling four state variables through three dynamical regimes. The system requires no continuum limit, no external drive, and no infinite-resource assumption (section 2).

2. **Three rigorous guarantees.** We prove that energy decreases monotonically, that total activity is almost surely finite, and that the system absorbs in finite time with probability one. Together, these establish an intrinsic thermodynamic arrow and guaranteed termination (section 3).

3. **Embedded phase transition.** A Landau free-energy functional governs bond formation, embedding a Landau-type local order–disorder transition within the cascade dynamics and producing a four-level structural hierarchy (section 2.9).

4. **Phase diagram and complexity peak.** We identify the principal regions of a phase diagram over initial energy density and interaction strength, and characterise a transient complexity peak where structural diversity first rises through explosive cascades before decaying toward absorption (section 4).

Scope of claims. All results in this paper concern the specific model class defined in section 2: a discrete-time, discrete-state stochastic process on a finite graph with a finite, non-renewable energy field. We do not claim generality beyond this class. The guarantees (monotonicity, finite activity, absorption) are theorems about this system; the phase diagram is qualitative; and the numerical illustrations are observations about dynamical regimes, not claims of physical equivalence to any natural system.

1.4 Organisation

Section 2 defines the model. Section 3 states and proves the main theorems. Section 4 analyses the phase structure. Section 5 discusses emergent properties and interpretation. Section 6 places the work in context and identifies open problems.

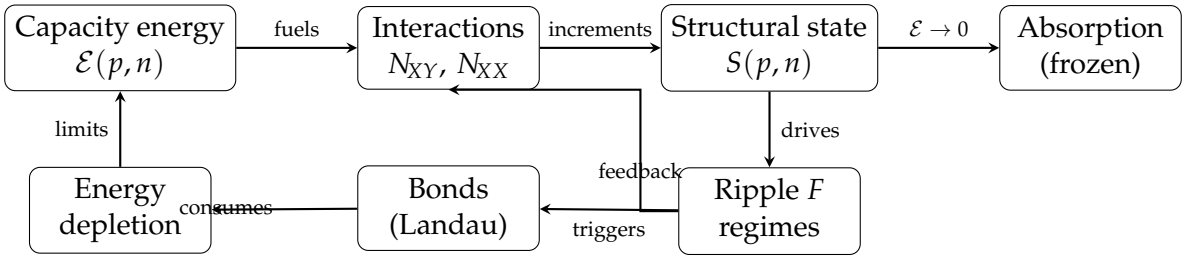

Figure 1: Conceptual flow of the discrete cascade dynamics. Energy fuels interactions, which build structure. Structure drives the ripple measure, which governs regime switching and bond formation. Bonds and interactions consume energy, creating a feedback loop that terminates when energy is exhausted (absorption).

2 Model Definition

2.1 Graph Topology

Definition 2.1 (Spatial substrate)**.** Let $\mathcal{G} = (\mathcal{V}, \mathcal{A})$ be a finite, connected, undirected graph with vertex set $\mathcal{V}$, $|\mathcal{V}| = P < \infty$, and adjacency relation $\mathcal{A} \subseteq \mathcal{V} \times \mathcal{V}$. For each vertex $p \in \mathcal{V}$ the *neighbourhood* is $\mathcal{N}(p) = \{q \in \mathcal{V} : (p,q) \in \mathcal{A}\}$, with degree $\deg(p) = |\mathcal{N}(p)|$.

Remark 2.2. The graph $\mathcal{G}$ may be a regular lattice ($\mathbb{Z}^d$ with periodic boundary conditions), a random graph, or any finite connected graph. Results in section 3 hold for arbitrary $\mathcal{G}$.

2.2 State Variables

At each vertex $p \in \mathcal{V}$ and discrete time step $n \in \mathbb{N}_0$, the system carries four state variables:

Definition 2.3 (Local state)**.** The *state* at vertex p and time n is the tuple

$$\sigma(p,n) = \big(X(p,n),\ Y(p,n),\ \mathcal{E}(p,n),\ S(p,n)\big) \ \in\ \mathbb{N}_0 \times \mathbb{N}_0 \times \mathbb{R}_{\geq 0} \times \mathbb{R}\,,$$

where:

- $X(p,n) \in \mathbb{N}_0$: count of *type-X excitations* (species 1), with intrinsic frequency $\omega_X > 0$,
- $Y(p,n) \in \mathbb{N}_0$: count of *type-Y excitations* (species 2), with intrinsic frequency $\omega_Y > 0, \omega_Y \neq \omega_X$,
- $\mathcal{E}(p,n) \in \mathbb{R}_{\geq 0}$: *local capacity energy*,
- $S(p,n) \in \mathbb{R}$: *structural state*, encoding accumulated interaction history and bonded configurations.

The two species are *fundamentally asymmetric*: they carry different intrinsic frequencies, obey different self-interaction rules (see section 2.4), and are not interchangeable under any symmetry of the model.

The *global state* at time n is the collection $\Sigma(n) = \{\sigma(p,n)\}_{p\in\mathcal{V}}$.

Definition 2.4 (Total capacity energy)**.**

$$\mathcal{E}_{\text{tot}}(n) \;=\; \sum_{p\in\mathcal{V}} \mathcal{E}(p,n)\,.$$

2.3 Parameters

The model is governed by the following constants:

Symbol	Name	Constraint
ω_X, ω_Y	Intrinsic frequencies	$\omega_X, \omega_Y > 0, 0 < \lvert\omega_X - \omega_Y\rvert < 2\pi$
ϑ	Coherence floor	$\vartheta \in (0,1]$
α_{XY}	Cross-interaction coefficient	$\alpha_{XY} > 0$
α_{XX}	X self-interaction coefficient	$\alpha_{XX} \geq 0$
k_{XY}	Energy cost per XY interaction	$k_{XY} > 0$
k_{XX}	Energy cost per XX interaction	$k_{XX} > 0$
C	Ripple threshold	$C > 0$
Δ	Overshoot margin	$\Delta > 0$
λ	Leakage rate	$\lambda > 0$
D_X, D_Y	Diffusion coefficients	$D_X, D_Y \in [0, 1/\deg_{\max})$
γ_1, γ_2	Structural coupling	$\gamma_1, \gamma_2 > 0$
γ_{XX}	XX structural coupling	$\gamma_{XX} \geq 0$
a_0	Free-energy linear coefficient	$a_0 > 0$
b	Free-energy quartic stabiliser	$b > 0$
T_c	Critical temperature for bonding	$T_c > 0$
κ	Energy cost per bond	$\kappa > 0$
η	Energy cost per explosion	$\eta > 0$

2.4 Interaction Dynamics

The two species obey *asymmetric* interaction rules: X excitations interact both with Y excitations (cross-interaction) and with other X excitations (self-interaction), while Y excitations interact *only* with X. The Y–Y channel is forbidden.

Definition 2.5 (Interaction rules and asymmetry)**.** At each vertex p and time step n, three interaction channels are evaluated:

(i) Cross-interaction (X–Y). Each species carries an intrinsic phase advancing at its frequency,

$$\phi_X(n) = \omega_X\, n\,, \qquad \phi_Y(n) = \omega_Y\, n\,,$$

and the efficiency of cross-interaction depends on the instantaneous phase alignment of the two species through the *interference factor*

$$\Theta(n) \;=\; \vartheta + (1-\vartheta)\,\frac{1+\cos\big(\phi_X(n) - \phi_Y(n)\big)}{2} \;=\; \vartheta + (1-\vartheta)\,\frac{1+\cos\big((\omega_X - \omega_Y)\,n\big)}{2} \;\in\; [\vartheta,\,1]\,, \tag{1}$$

where $\vartheta \in (0, 1]$ is the *coherence floor*: phase alignment modulates the efficiency of the cross-channel but never switches it off entirely. Since time is discrete, the frequency difference is interpreted modulo 2π; we assume $0 < |\omega_X - \omega_Y| < 2\pi$. The expected cross-interaction rate is

$$R_{XY}(p,n) = \alpha_{XY}\,\omega_X\,\omega_Y\,\Theta(n)\,X(p,n)\,Y(p,n)\,.$$

The realised count is $N_{XY}(p,n) \sim \mathrm{Poi}\big(R_{XY}(p,n)\big)$, capped at $\min\{X(p,n),\, Y(p,n)\}$. Each cross-interaction annihilates one X and one Y:

$$X(p,n) \;\leftarrow\; X(p,n) - N_{XY}(p,n)\,, \tag{2}$$
$$Y(p,n) \;\leftarrow\; Y(p,n) - N_{XY}(p,n)\,. \tag{3}$$

(ii) Self-interaction (X–X). Both participants in a self-interaction carry the same phase $\phi_X(n)$, so their phase difference vanishes identically and the interference factor equals 1: the self-channel is unmodulated. The expected X self-interaction rate is

$$R_{XX}(p,n) = \alpha_{XX}\,\omega_X^2\,\frac{X(p,n)\big(X(p,n)-1\big)}{2}\,,$$

counting unordered pairs. The realised count is $N_{XX}(p,n) \sim \mathrm{Poi}\big(R_{XX}(p,n)\big)$, capped at $\lfloor X(p,n)/2 \rfloor$. Each self-interaction annihilates two X excitations:

$$X(p,n) \;\leftarrow\; X(p,n) - 2\,N_{XX}(p,n)\,. \tag{4}$$

(iii) Y–Y interaction: forbidden. No Y–Y interactions occur:

$$N_{YY}(p,n) = 0 \qquad \text{for all } p,\, n\,. \tag{5}$$

All interaction counts are conditionally independent across vertices and channels given $\Sigma(n)$.

Remark 2.6 (Source of asymmetry)**.** The asymmetry $\alpha_{XX} \geq 0$, $\alpha_{YY} = 0$ is a *constitutive* property of the two species, not a consequence of dynamics. Combined with the distinct intrinsic frequencies $\omega_X \neq \omega_Y$, this makes the species genuinely non-interchangeable: the model has no $X \leftrightarrow Y$ symmetry. This asymmetry is the minimal structural assumption needed for the emergent hierarchy described in section 5.2.

Remark 2.7 (Why the interference factor is essential)**.** Without $\Theta(n)$, the frequencies would enter the dynamics only through the static products $\alpha_{XY}\omega_X\omega_Y$ and $\alpha_{XX}\omega_X^2$, and could therefore be absorbed entirely into the coupling constants: any model with $\omega_X \neq \omega_Y$ would be reproduced exactly by a model with equal frequencies and rescaled couplings, making the frequency mismatch dynamically vacuous. The interference factor breaks this degeneracy: the cross-channel efficiency oscillates with *beat period* $2\pi/|\omega_X - \omega_Y|$, which no rescaling of couplings can reproduce. This modulation is the mechanism by which frequency mismatch sustains the ripple $F = |\Delta^2 S|$, and it is the subject of the necessity theorem in Part II [Goswami, 2026b]. When $\omega_X = \omega_Y$, the factor reduces to the constant $\Theta \equiv 1$ and the model degenerates to the frequency-symmetric case.

2.5 Energy Depletion

Every interaction irreversibly consumes capacity energy.

Definition 2.8 (Energy cost of interaction)**.** The total energy depleted by interactions at vertex p is

$$\mathcal{C}_{\text{int}}(p,n) = k_{XY} \cdot N_{XY}(p,n) + k_{XX} \cdot N_{XX}(p,n)\,.$$

Remark 2.9. Energy is *consumed by* interactions, not released into the capacity field. The capacity field $\mathcal{E}$ acts as a finite fuel reserve that is irreversibly spent. The distinct costs k_{XY} and k_{XX} allow cross- and self-interactions to have different thermodynamic weights.

2.6 Ripple Measure

Definition 2.10 (Ripple intensity)**.** For $n \geq 2$, define the *ripple intensity* at vertex p as the discrete second-order temporal variation of the structural state:

$$F(p,n) = \left|S(p,n) - 2\,S(p,n{-}1) + S(p,n{-}2)\right|.$$

For $n < 2$, set $F(p,n) = 0$.

Equivalently, $F(p,n) = |\Delta^2 S(p,n)|$, the discrete second difference of S in time. The ripple intensity measures the magnitude of oscillatory change in structural state, a proxy for local dynamical volatility.

2.7 Regime Classification

The ripple intensity classifies each vertex into one of three regimes at each time step.

Definition 2.11 (Dynamical regimes)**.** At vertex p, time n:

R1. **Quiescent regime:** $F(p,n) \leq C$. No leakage, no explosion. The leakage and explosion contributions are zero: $L(p,n) = 0$, $M(p,n) = 0$.

R2. **Leakage regime:** $C < F(p,n) < C + \Delta$. Slow dissipation:

$$L(p,n) = \lambda\, F(p,n)\,.$$

No explosion: $M(p,n) = 0$.

R3. **Explosive regime:** $F(p,n) \geq C + \Delta$. An explosion event occurs:

$$m(p,n) = \left\lfloor \frac{F(p,n) - C}{\Delta} \right\rfloor, \tag{6}$$

$$M(p,n) = \eta \cdot m(p,n)\,, \tag{7}$$

where $m(p,n)$ is the number of new XY pairs created and $M(p,n)$ is the energy consumed. The pair creation is:

$$X(p,n{+}1) \;\leftarrow\; X(p,n{+}1) + m(p,n)\,, \tag{8}$$

$$Y(p,n{+}1) \;\leftarrow\; Y(p,n{+}1) + m(p,n)\,. \tag{9}$$

Explosion occurs only if $\mathcal{E}(p,n) \geq M(p,n)$; otherwise, m is reduced to the maximum affordable: $m(p,n) = \lfloor \mathcal{E}(p,n)/\eta \rfloor$. Leakage also applies: $L(p,n) = \lambda\, F(p,n)$.

Remark 2.12. The explosion count m in (6) grows linearly with the overshoot $F - C$, and each created pair costs energy η. This ensures that explosions are self-limiting: they drain the local energy reserve, reducing future explosion capacity.

2.8 Spatial Coupling

Excitations undergo nearest-neighbour diffusion on $\mathcal{G}$.

Definition 2.13 (Excitation diffusion)**.** After interaction and regime updates, excitations diffuse:

$$X(p, n+1) \leftarrow X(p, n+1) + D_X \sum_{q \in \mathcal{N}(p)} \big[X(q, n) - X(p, n)\big], \tag{10}$$

$$Y(p, n+1) \leftarrow Y(p, n+1) + D_Y \sum_{q \in \mathcal{N}(p)} \big[Y(q, n) - Y(p, n)\big]. \tag{11}$$

Values are rounded to the nearest non-negative integer. The constraint $D_X < 1/\deg_{\max}$ ensures that diffusion does not create negative counts in the continuous relaxation.

Remark 2.14. Diffusion is *conservative*: it redistributes excitations without creating or destroying them. Formally, $\sum_p X(p, n)$ is invariant under the diffusion step alone (up to rounding). The capacity energy $\mathcal{E}$ does *not* diffuse; it remains a local, immobile resource.

2.9 Bond Formation via Free-Energy Minimisation

We model bond formation as a local phase transition using a Landau free-energy functional [Landau, 1937].

Remark 2.15 (Justification of the Landau approach)**.** The Landau free energy is an equilibrium construct, and its application in a non-equilibrium, discrete stochastic system requires justification. We rely on a *timescale separation* argument. Bond formation at a vertex p depends on the local order parameter $\psi(p, n)$ and the effective temperature $T_{\text{eff}}(p, n)$, both of which are determined by the current state $\Sigma(p, n)$. Between successive global update steps, the local state at p is fixed; the Landau functional $\mathcal{F}(\psi)$ is therefore evaluated at a *frozen snapshot* of the local configuration. The stochastic evolution of ψ and T_{eff} over time is handled by the global update rule, not by the Landau functional itself. In this sense, the Landau functional serves as a *static decision rule* (form a bond if the free-energy gradient is favourable) rather than a dynamical equation of motion. This is analogous to how nucleation theory applies an equilibrium free-energy barrier to a non-equilibrium process: the barrier calculation is static, while the arrival of fluctuations that overcome it is stochastic. The key mathematical requirement is only that $\mathcal{F}$ be evaluated at well-defined, non-negative arguments ($\psi \geq 0$, $T_{\text{eff}} \geq 0$), which is guaranteed by theorem 3.1.

Definition 2.16 (Order parameter)**.** The *bond order parameter* at vertex p is

$$\psi(p, n) = \sqrt{X(p, n) \cdot Y(p, n)},$$

measuring the geometric co-density of the two excitation species.

Definition 2.17 (Effective temperature)**.**

$$T_{\text{eff}}(p,n) = \frac{F(p,n)}{C},$$

the normalised ripple intensity. High ripple corresponds to high effective temperature (disordered); low ripple to low temperature (ordered).

Definition 2.18 (Landau free energy)**.** The local *bond free energy* is

$$\mathcal{F}(\psi) = a_0\big(T_{\text{eff}} - T_c\big)\,\psi^2 + b\,\psi^4\,. \tag{12}$$

Bond formation is thermodynamically favourable when the free-energy gradient with respect to ψ is negative:

$$\frac{\partial \mathcal{F}}{\partial \psi} = 2\,a_0(T_{\text{eff}} - T_c)\,\psi + 4b\,\psi^3 < 0\,.$$

For $\psi > 0$ this requires

$$T_{\text{eff}}(p,n) < T_c - \frac{2b}{a_0}\,\psi^2(p,n)\,, \tag{13}$$

i.e., sufficiently low ripple (ordered local state) and sufficiently high co-density.

Definition 2.19 (Bond formation rate)**.** The number of bonds formed at vertex p is

$$B(p,n) = \begin{cases} \min\left(\left\lfloor \psi^2(p,n)\cdot\dfrac{|\partial\mathcal{F}/\partial\psi|}{b}\right\rfloor,\ \left\lfloor\dfrac{\mathcal{E}(p,n)}{\kappa}\right\rfloor,\ X(p,n),\ Y(p,n)\right) & \text{if (13) holds,} \\ 0 & \text{otherwise.} \end{cases} \tag{14}$$

Each bond:

- removes one X and one Y excitation from the free population,
- consumes energy κ from $\mathcal{E}(p,n)$,
- contributes $+\gamma_2$ to the structural state $S(p,n{+}1)$.

Bonds are *metastable*: they persist in S but obey the same ripple and energy rules as free excitations. In particular:

- A bonded vertex carries reduced capacity energy ($\mathcal{E}$ diminished by κ at formation).
- If a subsequent explosion at or near the bonded vertex raises F above $C + \Delta$, the bond may be disrupted: the structural contribution persists in S, but new excitations created by the explosion can overwhelm the local ordered phase.
- Bonds can therefore *form, persist, and later decay* through the same threshold mechanism that governs free excitations.

Terminological clarification. "Bond decay" refers to the disruption of the local *ordered phase* that a bond represents, not to a decrement of any state variable: the model does not track a count of currently intact bonds, and the structural state S (which records the cumulative history of bond formation) is monotone non-decreasing by construction (section 2.10). A bond is an event whose ordered context can be destroyed by subsequent explosions; its historical trace in S persists. Tracking intact bonds as a separate decrementable variable would be a natural model extension but is not required for any result in this paper.

Remark 2.20. The quartic term $b\,\psi^4$ in (12) prevents unbounded bond formation. The condition $T_{\text{eff}} < T_c$ defines a Landau-type order–disorder transition at the local level: bonds form in the "ordered" (low ripple) phase and dissolve in the "disordered" (high ripple) phase. The fact that bonds are subject to the same dynamical rules as free excitations, rather than being permanent, is essential: it means the structural hierarchy (see section 5.2) is itself transient and history-dependent.

2.10 Structural State Evolution

Definition 2.21 (S update)**.**

$$S(p,n{+}1) = S(p,n) + \gamma_1\, N_{XY}(p,n) + \gamma_{XX}\, N_{XX}(p,n) + \gamma_2\, B(p,n)\,. \tag{15}$$

The structural state accumulates the history of all interactions (cross and self) and bonds. It has no decay term: once structure is created, it persists (though its influence via the ripple measure may diminish as the system freezes).

2.11 Complete Update Rule

The full time-step $n \to n{+}1$ proceeds in the following deterministic order:

1. **Interaction:** Sample $N_{XY}(p,n)$ and $N_{XX}(p,n)$ for all p per theorem 2.5. Annihilate excitations via (2)–(4).
2. **Ripple computation:** Compute $F(p,n)$ for all p.
3. **Regime classification and leakage/explosion:** Apply theorem 2.11. Create new excitations if explosive.
4. **Bond formation:** Compute ψ, T_{eff}, $\mathcal{F}$, and form bonds via theorem 2.19.
5. **Energy update:**

$$\mathcal{E}(p,n{+}1) = \mathcal{E}(p,n) - \underbrace{k_{XY}\cdot N_{XY}(p,n) + k_{XX}\cdot N_{XX}(p,n)}_{\text{interaction costs}} - \underbrace{L(p,n)}_{\text{leakage}} - \underbrace{M(p,n)}_{\text{explosion cost}} - \underbrace{\kappa\cdot B(p,n)}_{\text{bond cost}}, \tag{16}$$

   clamped to $\max(\cdot,0)$. Summing over all vertices, $\mathcal{E}_{\text{tot}}(n+1) \le \mathcal{E}_{\text{tot}}(n)$, with strict inequality whenever at least one site has positive cost at step n; see theorem 3.3.
6. **Structural update:** Apply (15).
7. **Diffusion:** Apply (10)–(11).

Definition 2.22 (Absorbing state)**.** A configuration Σ is *absorbing* if, for all $p \in \mathcal{V}$:

$$X(p)\cdot Y(p) = 0\,, \qquad X(p) \le 1 \;\; (\text{if } \alpha_{XX} > 0)\,, \qquad F(p) \le C\,.$$

The first two conditions ensure no cross- or self-interactions can occur; the third ensures no leakage or explosions. In an absorbing state $\Sigma(n) = \Sigma(n{+}1)$ for all subsequent n.

3 Main Results

Throughout this section, let $(\Sigma(n))_{n\geq 0}$ be the Markov chain defined by the update rule in section 2.11 on the filtered probability space $(\Omega, \mathcal{F}, (\mathcal{F}_n)_{n\geq 0}, \mathbb{P})$, where $\mathcal{F}_n = \sigma(\Sigma(0), \ldots, \Sigma(n))$. Because the interference factor $\Theta(n)$ in (1) is a deterministic function of the step index, the chain is time-inhomogeneous; equivalently, the pair $(\Sigma(n), n)$ is a homogeneous Markov chain. None of the results below rely on time-homogeneity: all bounds use only $\Theta(n) \geq \vartheta$.

3.1 Well-Posedness

Proposition 3.1 (Well-posedness)**.** *For any initial configuration $\Sigma(0)$ with $X(p,0), Y(p,0) \in \mathbb{N}_0$, $\mathcal{E}(p,0) \geq 0$, and $S(p,0) \in \mathbb{R}$ for all $p \in \mathcal{V}$, the update rule preserves these domains: for all $n \geq 0$,*

$$X(p,n) \in \mathbb{N}_0, \quad Y(p,n) \in \mathbb{N}_0, \quad \mathcal{E}(p,n) \geq 0, \quad S(p,n) \in \mathbb{R}\,.$$

Proof. Excitation non-negativity. Interaction counts N_{XY} and bond counts B are capped at $\min(X, Y)$, so the annihilation step cannot drive X or Y below zero. For diffusion, the parameter constraint $D_X < 1/\deg_{\max}$ guarantees that the outflow from any vertex p satisfies $D_X \sum_{q\sim p} X(p) = D_X \deg(p)\, X(p) \leq D_X \deg_{\max} X(p) < X(p)$, so after rounding to $\mathbb{N}_0$ the post-diffusion count remains non-negative; the same argument applies to Y with D_Y.

Energy non-negativity. The clamp $\mathcal{E}(p,n+1) \leftarrow \max\big(\mathcal{E}(p,n+1),\, 0\big)$ in step 5 of the update rule enforces $\mathcal{E}(p,n) \geq 0$ for all p, n.

Structural state. S evolves by addition of non-negative terms ($\gamma_1 N_{XY}$, $\gamma_{XX} N_{XX}$, $\gamma_2 B$, all ≥ 0) and remains in $\mathbb{R}$. □

3.2 Energy Monotonicity

Definition 3.2 (Total depletion)**.**

$$\mathcal{D}(n) = \sum_{p\in\mathcal{V}} \left[k_{XY}\, N_{XY}(p,n) + k_{XX}\, N_{XX}(p,n) + L(p,n) + M(p,n) + \kappa\, B(p,n)\right].$$

Theorem 3.3 (Energy Monotonicity)**.** *The total capacity energy $\mathcal{E}_{\text{tot}}(n)$ satisfies:*

(a) $\mathcal{E}_{\text{tot}}(n+1) = \mathcal{E}_{\text{tot}}(n) - \mathcal{D}(n)$ *for all $n \geq 0$.*

(b) $\mathcal{D}(n) \geq 0$ *almost surely, hence $\mathcal{E}_{\text{tot}}(n+1) \leq \mathcal{E}_{\text{tot}}(n)$ a.s.*

(c) $\mathbb{E}[\mathcal{D}(n) \mid \mathcal{F}_n] > 0$ *whenever $\Sigma(n)$ is not absorbing.*

Consequently, $\big(\mathcal{E}_{\text{tot}}(n)\big)_{n\geq 0}$ is a non-negative supermartingale.

Proof. **(a)** Summing (16) over all $p \in \mathcal{V}$:

$$\mathcal{E}_{\text{tot}}(n+1) = \sum_p \mathcal{E}(p,n+1)$$

$$= \sum_p \Big[\mathcal{E}(p,n) - k_{XY}\, N_{XY}(p,n) - k_{XX}\, N_{XX}(p,n) - L(p,n) - M(p,n) - \kappa\, B(p,n)\Big] = \mathcal{E}_{\text{tot}}(n) - \mathcal{D}(n)\,.$$

(The clamp to zero can only further reduce the sum, strengthening the inequality.)

(b) Each term in $\mathcal{D}(n)$ is a product of a positive constant and a non-negative count or rate. Hence $\mathcal{D}(n) \geq 0$.

(c) Suppose $\Sigma(n)$ is not absorbing. Then at least one of the following holds:

- There exists p with $X(p,n) \geq 1$ and $Y(p,n) \geq 1$. Then $R_{XY}(p,n) = \alpha_{XY}\,\omega_X\omega_Y\,\Theta(n)\,X\,Y \geq \alpha_{XY}\omega_X\omega_Y\vartheta > 0$ (using $\Theta(n) \geq \vartheta$), so $\mathbb{E}[k_{XY}\,N_{XY}(p,n)] > 0$.
- There exists p with $X(p,n) \geq 2$ and $\alpha_{XX} > 0$. Then $R_{XX}(p,n) \geq \alpha_{XX}\,\omega_X^2 > 0$, so $\mathbb{E}[k_{XX}\,N_{XX}(p,n)] > 0$.
- $F(p,n) > C$ for some p, giving $L(p,n) = \lambda\,F(p,n) > \lambda\,C > 0$.

In every case $\mathbb{E}[\mathcal{D}(n) \mid \mathcal{F}_n] > 0$.

Since $\mathcal{E}_{\text{tot}}(n) \geq 0$ and $\mathbb{E}[\mathcal{E}_{\text{tot}}(n+1) \mid \mathcal{F}_n] = \mathcal{E}_{\text{tot}}(n) - \mathbb{E}[\mathcal{D}(n) \mid \mathcal{F}_n] \leq \mathcal{E}_{\text{tot}}(n)$, the process $\big(\mathcal{E}_{\text{tot}}(n)\big)$ is a non-negative supermartingale. □

3.3 Finite Activity Bound

Theorem 3.4 (Finite Activity Bound)**.** *The total number of interactions, leakage events, explosion events, and bond formations across all space and time is almost surely finite. Specifically:*

$$\sum_{n=0}^{\infty}\sum_{p\in\mathcal{V}} N_{XY}(p,n) \;\leq\; \frac{\mathcal{E}_{\text{tot}}(0)}{k_{XY}} \qquad \text{a.s.} \tag{17}$$

More generally,

$$\sum_{n=0}^{\infty}\mathcal{D}(n) \leq \mathcal{E}_{\text{tot}}(0) \qquad \text{a.s.} \tag{18}$$

Proof. From theorem 3.3(a), telescoping:

$$\mathcal{E}_{\text{tot}}(N) = \mathcal{E}_{\text{tot}}(0) - \sum_{n=0}^{N-1}\mathcal{D}(n)\,.$$

Since $\mathcal{E}_{\text{tot}}(N) \geq 0$ for all N:

$$\sum_{n=0}^{N-1}\mathcal{D}(n) \leq \mathcal{E}_{\text{tot}}(0)\,.$$

Taking $N \to \infty$ and using the monotone convergence theorem:

$$\sum_{n=0}^{\infty}\mathcal{D}(n) \leq \mathcal{E}_{\text{tot}}(0) < \infty\,.$$

Since $k_{XY}\,N_{XY}(p,n) \leq \mathcal{D}(n)$ for each p, inequality (17) follows by extracting the cross-interaction term (with $k = k_{XY}$). Analogous bounds hold for X–X interactions ($\leq \mathcal{E}_{\text{tot}}(0)/k_{XX}$), total leakage ($\leq \mathcal{E}_{\text{tot}}(0)/\lambda C$), total explosions ($\leq \mathcal{E}_{\text{tot}}(0)/\eta$), and total bonds ($\leq \mathcal{E}_{\text{tot}}(0)/\kappa$). □

Corollary 3.5. *The system generates at most* $\lfloor \mathcal{E}_{\text{tot}}(0)/\min(k_{XY}, k_{XX}, \eta, \kappa)\rfloor$ *total events across its entire history.*

3.4 Almost Sure Absorption

Theorem 3.6 (Almost Sure Absorption)**.** *There exists an almost surely finite random time $\tau < \infty$ such that $\Sigma(n)$ is absorbing for all $n \geq \tau$:*

$$\mathbb{P}\big(\exists\, \tau < \infty : \Sigma(n) \text{ is absorbing } \forall\, n \geq \tau\big) = 1\,.$$

Proof. We argue that activity cannot persist indefinitely.

Step 1. By theorem 3.4, $\sum_n \mathcal{D}(n) < \infty$ a.s. Since $\mathcal{D}(n) \geq 0$, we have $\mathcal{D}(n) \to 0$ a.s.

Step 2. Suppose for contradiction that the system is non-absorbing for infinitely many n. At each such n, by the proof of theorem 3.3(c), there exists a vertex p_n where either:

(i) $X(p_n, n) \geq 1$ and $Y(p_n, n) \geq 1$, or

(ii) $F(p_n, n) > C$.

Case (i): If $X(p_n, n) \geq 1$ and $Y(p_n, n) \geq 1$, then $R_{XY}(p_n, n) \geq \alpha_{XY}\omega_X\omega_Y\vartheta > 0$ (since $\Theta(n) \geq \vartheta$ uniformly in n) and $\mathbb{P}(N_{XY} \geq 1) \geq 1 - e^{-\alpha_{XY}\omega_X\omega_Y\vartheta} > 0$. When a cross-interaction occurs, $\mathcal{D}(n) \geq k_{XY} > 0$. If instead $X(p_n, n) \geq 2$ and $\alpha_{XX} > 0$, the same argument applies to N_{XX} with cost k_{XX}.

Let A_n be the event $\{\mathcal{D}(n) \geq k_{XY}\}$. Conditionally on $\mathcal{F}_n$, whenever case (i) holds at step n, the Poisson draw gives $\mathbb{P}(A_n \mid \mathcal{F}_n) \geq 1 - e^{-\alpha_{XY}\omega_X\omega_Y\vartheta} =: c > 0$. Since $\sum_n \mathbb{P}(A_n \mid \mathcal{F}_{n-1}) \geq c \cdot \#\{n : \text{case (i) holds}\} = \infty$ on the event that case (i) occurs infinitely often, the conditional Borel–Cantelli lemma (Lévy's extension; see, e.g., Liggett 1999, Appendix A) implies that infinitely many A_n occur a.s. on that event. Each occurrence contributes $\mathcal{D}(n) \geq k_{XY} > 0$, so $\sum_n \mathcal{D}(n) = \infty$ a.s., contradicting $\sum_n \mathcal{D}(n) < \infty$.

Case (ii): If $F(p_n, n) > C$ infinitely often, then $\mathcal{D}(n) \geq L(p_n, n) = \lambda\, F(p_n, n) > \lambda C > 0$ infinitely often, again contradicting $\mathcal{D}(n) \to 0$.

Step 3. Therefore, only finitely many non-absorbing steps occur. Let τ be the last such step; then $\Sigma(n)$ is absorbing for $n > \tau$. □

Remark 3.7 (Final configuration)**.** At absorption, the residual state consists of:

- residual excitations that are not co-located ($X \cdot Y = 0$ everywhere),
- residual capacity energy $\mathcal{E}(p, \tau) \geq 0$ (possibly positive),
- a frozen structural state $S(p, \tau)$ encoding the cumulative history of all interactions and bonds.

The final configuration depends on the entire stochastic history and is generically unique to each realisation. This *stochastic memory* of the last cascade is imprinted in the structural field.

Remark 3.8 (Why F_{avg} eventually decreases)**.** As total energy falls, total activity (interactions, explosions, bonds) must eventually fall. The increments to S therefore become smaller and less frequent. Since $F = |\Delta^2 S|$ is driven by those increments, their slowdown implies that the average ripple $F_{\text{avg}}(n)$ tends to decrease in the long run until $F \leq C$ everywhere and the system is quiescent.

3.5 Simulation

The dynamics were implemented in Python (see section A, the `model_simulation` folder, and section 3.7 for computational complexity analysis). Figure 2 shows a typical run: total capacity energy decreases monotonically (theorem 3.3), excitations X and Y evolve asymmetrically until activity ceases, and the mean ripple F_{avg} rises then falls as structure builds and the system approaches absorption.

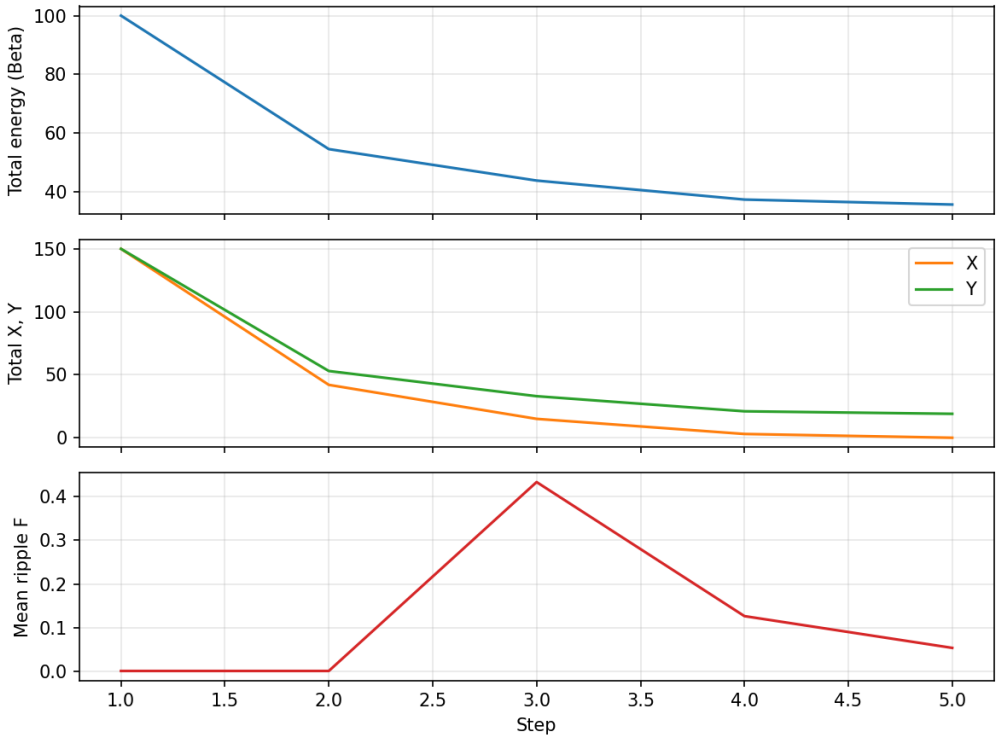

Figure 2: Simulation run on a periodic chain of $P = 50$ sites: initial $X = Y = 3$, $\mathcal{E}_{\text{tot}}(0) = 100$, default parameters. **Top:** total capacity energy (strictly decreasing). **Middle:** total X and Y (asymmetric depletion). **Bottom:** mean ripple F. Generated by `model_simulation/run_simulation.py`.

3.6 Convergence Rate

Proposition 3.9 (Expected absorption time bound)**.** *Let*

$$c_0 = 1 - e^{-\alpha_{XY}\omega_X\omega_Y\vartheta}, \qquad c_1 = 1 - e^{-\alpha_{XX}\omega_X^2} \ \text{(when } \alpha_{XX} > 0\text{)},$$

and define the uniform depletion constant

$$\delta^* = \begin{cases} \min\left(k_{XY}\, c_0,\ k_{XX}\, c_1,\ \lambda\, C,\ \eta\right) & \text{if } \alpha_{XX} > 0, \\ \min\left(k_{XY}\, c_0,\ \lambda\, C,\ \eta\right) & \text{if } \alpha_{XX} = 0, \end{cases}$$

which is strictly positive in either case. Then the expected time to absorption satisfies

$$\mathbb{E}[\tau] \ \le\ 3\left(\frac{\mathcal{E}_{\text{tot}}(0)}{\delta^*} + 1\right).$$

Proof. Partition time into consecutive windows of three steps and consider any window whose first step n finds $\Sigma(n)$ non-absorbing. By theorem 2.22, at least one of the following holds at step n.

Case (i): $X(p,n)\,Y(p,n) \geq 1$ for some p. Then $R_{XY}(p,n) \geq \alpha_{XY}\omega_X\omega_Y\vartheta$ (using $\Theta(n) \geq \vartheta$), so a cross-interaction occurs at p with probability at least c_0, each depleting at least k_{XY}. Hence $\mathbb{E}[\mathcal{D}(n) \mid \mathcal{F}_n] \geq k_{XY}\,c_0 \geq \delta^*$.

Case (ii): $X(p,n) \geq 2$ for some p and $\alpha_{XX} > 0$. Analogously, $\mathbb{E}[\mathcal{D}(n) \mid \mathcal{F}_n] \geq k_{XX}\,c_1 \geq \delta^*$.

Case (iii): neither (i) nor (ii), but $F(p,n) > C$ for some p. With no co-located pairs and no self-interaction pairs anywhere, no interactions or bonds occur, so the structural field satisfies $S(\cdot, n{+}1) = S(\cdot, n)$. At each vertex with $F > C$, one of three things happens: (a) leakage or explosion depletes at least $\min(\lambda C, \eta)$ of local energy, giving $\mathbb{E}[\mathcal{D}(n) \mid \mathcal{F}_n] \geq \delta^*$; (b) an explosion creates new excitation pairs, in which case Case (i) or (ii) applies at step $n{+}1$ and $\mathbb{E}[\mathcal{D}(n{+}1) \mid \mathcal{F}_{n+1}] \geq \delta^*$; or (c) the local energy reserve is too depleted to fund either, in which case no structural increment occurs at any vertex during the window, so $F(\cdot, n{+}2) = 0$ and, absent new excitations, the configuration is absorbing by step $n{+}2$.

Thus every three-step window that begins non-absorbed either ends absorbed (which, by the argument in Case (iii)(c), can happen for at most one window without the δ^* depletion guarantee) or contributes expected depletion at least δ^*. Since total depletion is bounded by $\mathcal{E}_{\text{tot}}(0)$ (theorem 3.4), the expected number of windows that begin non-absorbed is at most $\mathcal{E}_{\text{tot}}(0)/\delta^* + 1$, and therefore $\mathbb{E}[\tau] \leq 3\,(\mathcal{E}_{\text{tot}}(0)/\delta^* + 1)$. □

Remark 3.10. The constant δ^* is uniform over all reachable configurations: it does not depend on how excitations are arranged, only on the model parameters. An earlier draft used a constant computed from the *initial* co-location pattern $\min_{p:XY>0} X(p,0)Y(p,0)$; that quantity is not a valid per-step lower bound, because co-location counts evolve and can temporarily vanish. The window argument above repairs this: it covers configurations in which activity is latent (elevated ripple with separated excitations) by tracking the forced resolution of such states within two further steps. The coherence floor $\vartheta > 0$ in the interference factor (1) guarantees that phase misalignment can slow the cross-channel but never suspend it.

3.7 Computational Complexity of Simulations

Remark 3.11 (Complexity Summary)**.** Each simulation step scales linearly with system size ($\mathcal{O}(P)$), and total expected runtime is bounded by the initial total energy ($\mathcal{O}(\mathcal{E}_{\text{tot}}(0) \cdot P)$).

This linear scaling ensures that simulation results reported in subsequent sections are not artefacts of computational constraints but reflect intrinsic system dynamics.

The computational exploration of the discrete cascade model (section 3.5) is implemented via simulation of the update rules defined in section 2. We analyse the space and time complexity of the core update loop with respect to the number of vertices P, the maximum graph degree d, and the initial capacity energy $\mathcal{E}_{\text{tot}}(0)$.

Space Complexity. The state space requires storing arrays for the primary variables X, Y, $\mathcal{E}$, S, and B at each vertex. The ripple calculation $F = |\Delta^2 S|$ requires a structural

history of depth 3. All intermediate variables (e.g., N_{XY}, N_{XX}, L, M) are evaluated and overwritten per step. Thus, the memory footprint scales strictly linearly with the graph size. The space complexity is $\mathcal{O}(P)$ per step. Storing the full history for post-run analysis requires $\mathcal{O}(\tau \cdot P)$, which scales linearly and remains tractable for large P under typical conditions.

Time Complexity (Per Step). The update rule decomposes into local operations and spatial transport.

1. **Local updates:** The interaction rates, Poisson sampling, ripple evaluation, regime switching, and structural/energy increments are pointwise operations. These are evaluated across all P vertices simultaneously via vectorised array operations, yielding $\mathcal{O}(P)$ time complexity.
2. **Spatial transport:** Diffusion requires passing excitation counts along edges. For general graphs with bounded maximum degree d, this operation requires $\mathcal{O}(d \cdot P)$ time. On the 1D chain topology used in our standard simulations ($d = 2$), diffusion is implemented via array shifts (e.g., `np.roll`), which maintain $\mathcal{O}(P)$ complexity. For sparse graphs with bounded degree, d is constant; for dense graphs, d may scale with P, increasing complexity accordingly.

The time complexity per step is $\mathcal{O}(d \cdot P)$.

Total Time Complexity (Full Run). The total execution time depends on the number of steps τ required for the system to reach the absorbing frozen state. As established in theorem 3.9, the expected absorption time satisfies $\mathbb{E}[\tau] \leq 3(\mathcal{E}_{\text{tot}}(0)/\delta^* + 1)$, implying that the number of effective update steps scales as $\mathcal{O}(\mathcal{E}_{\text{tot}}(0))$. Under the finite energy constraint, the total number of effective update steps is bounded by $\mathcal{O}(\mathcal{E}_{\text{tot}}(0))$, yielding an overall expected (in probability) time complexity of $\mathcal{O}(d \cdot \mathcal{E}_{\text{tot}}(0) \cdot P)$.

The simulation does not exhibit combinatorial or exponential scaling under the finite energy constraint. The runtime is intrinsically bounded by irreversible energy depletion, enabling efficient exploration of system behaviour even for large graphs and high-energy initial conditions.

4 Phase Structure and Transient Complexity

4.1 Phase Diagram

The qualitative behaviour of the system depends on two dimensionless control parameters:

Definition 4.1 (Control parameters)**.**

$$\rho_0 = \frac{1}{P} \sum_p X(p,0)\, Y(p,0) \qquad \text{(initial co-density)}\,, \tag{19}$$

$$\varepsilon_0 = \frac{\mathcal{E}_{\text{tot}}(0)}{P} \qquad \text{(initial energy density)}\,. \tag{20}$$

Theorem 4.2 (Phase classification)**.** *The model exhibits three qualitative phases depending on* (ρ_0, ε_0)*:*

1. ***Immediate absorption*** *($\varepsilon_0 < k_{\min}$ or $\rho_0 = 0$, where $k_{\min} = \min(k_{XY}, k_{XX})$). Insufficient energy or excitations for sustained activity. The system absorbs within $O(1)$ steps.*

2. ***Dissipative decay*** *($\varepsilon_0 \geq k_{\min}$, $\rho_0 > 0$, initial $F < C + \Delta$ everywhere). Interactions occur and deplete energy, but no explosions are triggered. Excitation density decays monotonically. The structural state grows monotonically until absorption.*

3. ***Cascade regime*** *($\varepsilon_0 \gg k_{\min}$, ρ_0 sufficient to generate $F \geq C + \Delta$). Explosions create new excitation pairs, sustaining and amplifying activity in transient bursts. The system passes through a complexity peak before eventual absorption.*

Proof sketch. Phase 1 is immediate from the energy bound: if $\mathcal{E}(p, 0) < k_{\min}$ for all p, no interaction can complete (each requires at least $k_{\min}$ energy), so $N_{XY} = N_{XX} = 0$ everywhere regardless of excitation counts.

Phase 2: without explosions, X and Y decrease monotonically (interactions and bonds only annihilate excitations). The number of interactions per step is bounded by $\min(X, Y)$, which is non-increasing. S grows by $\gamma_1 N_{XY} + \gamma_2 B \geq 0$.

Phase 3: explosions create excitations, which interact, which may increase F above the explosion threshold again, creating a cascade. But each cascade step costs energy (theorem 3.4), so the cascade is self-limiting. The total cascade duration is bounded by $\mathcal{E}_{\text{tot}}(0)/\eta$. □

4.2 Transient Complexity Peak

Definition 4.3 (Structural complexity)**.**

$$\mathcal{K}(n) = \frac{1}{P} \sum_{p \in \mathcal{V}} \left(S(p, n) - \bar{S}(n) \right)^2 , \qquad \bar{S}(n) = \frac{1}{P} \sum_{p} S(p, n) .$$

This is the spatial variance of the structural state, measuring heterogeneity of accumulated structure across the graph.

Proposition 4.4 (Complexity peak)**.** *In the cascade regime (theorem 4.2, Phase 3), the structural complexity $\mathcal{K}(n)$ satisfies:*

(a) $\mathcal{K}(0) = 0$ if $S(p, 0) = 0$ for all p.

(b) There exists $n^* > 0$ such that $\mathcal{K}(n^*) > 0$.

(c) $\mathcal{K}(n)$ is eventually constant (frozen at $\mathcal{K}(\tau)$).

Consequently, $\mathcal{K}$ has a non-trivial transient profile that first increases, may fluctuate, and ultimately freezes.

Proof. (a) is immediate. For (b), in the cascade regime at least one explosion occurs at some vertex p^* at some time n_1, adding excitations that produce $N_{XY}(p^*, n_1) > 0$ with positive probability. This increases $S(p^*, n_1{+}1)$ but not $S(q, n_1{+}1)$ for distant q, creating spatial variance. (c) follows from absorption: after τ, S is constant. □

4.3 Critical Threshold for Cascades

Proposition 4.5 (Cascade onset)**.** *A necessary condition for the cascade regime is:*

$$\gamma_1 \, \alpha_{XY} \, \omega_X \omega_Y \, \rho_0 + \gamma_{XX} \, \alpha_{XX} \, \omega_X^2 \, \bar{X}_0 \, (\bar{X}_0 - 1)/2 > C \, ,$$

where $\bar{X}_0$ is the mean initial X-count per vertex. That is, the expected structural increment from all interaction channels at initial density must exceed the ripple threshold.

Proof. For $F(p,n) > C$ at the earliest time $n = 2$, we need $|S(p,2) - 2S(p,1) + S(p,0)| > C$. If $S(p,0) = 0$, this requires $|S(p,2) - 2S(p,1)| > C$. Since $S(p,1) = \gamma_1 \, N_{XY}(p,0) + \gamma_{XX} \, N_{XX}(p,0)$ and the expected contributions scale as $\gamma_1 \, \alpha_{XY} \omega_X \omega_Y \, \rho_0$ and $\gamma_{XX} \, \alpha_{XX} \omega_X^2 \, \bar{X}_0 (\bar{X}_0 - 1)/2$ respectively, the expected magnitude of the second difference yields the stated condition. □

5 Emergent Properties and Interpretation

5.1 Layered Architecture

The model admits a natural decomposition into five conceptual layers, each emergent from the one below:

1. **Micro-field layer.** Stochastic X–Y and X–X interactions at individual vertices. The fundamental asymmetry ($\alpha_{YY} = 0$) and distinct frequencies $\omega_X \neq \omega_Y$ are the irreducible source of all dynamics.

2. **Energy layer.** Capacity energy $\mathcal{E}$ consumed per interaction. Provides the irreversible resource constraint.

3. **Instability control layer.** The ripple measure F and threshold C classify dynamics into quiescent, dissipative, and explosive regimes. This creates qualitative diversity from quantitative variation.

4. **Structural emergence layer.** Bond formation and structural state S create persistent, spatially heterogeneous configurations. These are the "fossils" of past activity.

5. **Thermodynamic arrow layer.** The monotonic decrease of $\mathcal{E}_{\text{tot}}$ imposes a global directionality on the dynamics. No time-reversal symmetry exists: the system has an intrinsic arrow.

5.2 Structural Hierarchy

The asymmetric interaction rules and bond formation produce a natural hierarchy of increasingly complex structures:

Level	Entity	Characteristics
0	Free excitation (X or Y)	Single species, mobile, reactive
1	Co-located pair (X + Y at same p)	Can interact, annihilate, or bond
2	Bond (X–Y composite in S)	Metastable, reduced $\mathcal{E}$, obeys same rules
3	Clump (cluster of bonds on $\mathcal{G}$)	Spatially extended, collective ripple

Each level emerges from the dynamics of the level below. Level-0 entities are placed by initial conditions and explosions. Level-1 co-locations arise from diffusion. Level-2 bonds form when the free-energy condition (13) is satisfied. Level-3 clumps form when neighbouring vertices independently satisfy the bonding condition, creating spatially correlated structural states.

The hierarchy is *transient*: clumps form, persist while local energy supports them, and ultimately freeze when the system absorbs. The frozen final state is not optimised, not symmetric, and not predictable from initial conditions alone; it is simply the arrested residue of the last cascade.

5.3 Thermodynamic Arrow

Corollary 5.1 (Irreversibility)**.** *The dynamics are time-irreversible. For any non-absorbing state* Σ*, the probability of returning to a state with higher total energy is exactly zero:*

$$\mathbb{P}\big(\mathcal{E}_{\text{tot}}(n{+}1) > \mathcal{E}_{\text{tot}}(n)\big) = 0 \qquad \forall\, n \geq 0\,.$$

This follows immediately from (16) and the non-negativity of all depletion terms. The system possesses a *strict thermodynamic arrow* without any need to invoke entropy or ergodic assumptions.

5.4 Stochastic Memory

The final frozen structural state $S(p, \tau)$ depends on the entire realisation of the stochastic process. Different runs from the same initial conditions produce generically different final configurations. This "stochastic memory" is a permanent record of the system's particular history, a discrete analogue of symmetry breaking in equilibrium phase transitions.

The absorbing configuration is not optimised with respect to any functional, not symmetric under any non-trivial automorphism of $\mathcal{G}$, and not reconstructible from the initial conditions alone. It is the arrested residue of the last cascade: a fossil record of the system's entire stochastic biography, frozen into the structural field when the energy ran out.

5.5 Self-Limiting Cascades

In the explosive regime, cascades are necessarily self-limiting. Each explosion creates new excitations (increasing future interaction potential) but costs energy (decreasing future capacity). The cascade terminates when either:

- local energy is exhausted ($\mathcal{E}(p) < \eta$), or
- created excitations diffuse and dilute below the interaction threshold.

This produces burst-like activity with heavy-tailed duration distributions, reminiscent of avalanche dynamics in SOC models, but guaranteed to eventually cease entirely.

5.6 Physical Interpretations and Analogies

In high-energy initial regimes, the cascade exhibits a transient phase of rapid activity, followed by the emergence of structured configurations and eventual irreversible decay toward an absorbing state. These qualitative features bear a loose analogy to large-scale processes such as rapid expansion, structure formation, and thermodynamic relaxation observed in physical systems.

We emphasize, however, that the present model is purely discrete and abstract, and no direct physical correspondence is claimed. Rather, such analogies are intended as conceptual interpretations that may guide future investigation into whether similar structural principles arise in more physically grounded settings.

6 Discussion

6.1 Relation to Existing Frameworks

Contact process and directed percolation. The contact process on a graph has a single species that can infect neighbours or recover. It exhibits a continuous phase transition between an absorbing state and an active steady state. Our model differs in four respects: (i) two *asymmetric* species with distinct frequencies and interaction rules, (ii) a global energy constraint that makes absorption *certain* rather than a phase boundary, (iii) structural memory that breaks the Markov property of the order parameter alone, and (iv) a structural hierarchy (excitation $\to$ pair $\to$ bond $\to$ clump) absent from single-species models. *Key distinction:* unlike the contact process, absorption here is guaranteed for all parameter values without fine-tuning to a critical point (theorem 3.6).

Sandpile models. The Abelian sandpile [Dhar, 1990] achieves criticality through slow external driving and fast relaxation (separation of timescales). Our model has no external drive; it runs on a finite endowment. The transient complexity peak (theorem 4.4) is analogous to the SOC steady state, but is inherently non-stationary and terminal. *Key distinction:* there is no external energy source; the complexity peak is a transient phenomenon bounded by the initial endowment (theorem 3.4).

Reaction–diffusion annihilation. The $A + B \to \varnothing$ system [Toussaint & Wilczek, 1983] on lattices shows anomalous kinetics (density decay $\sim t^{-d/4}$ in d dimensions). Our model extends this by adding an energy field, threshold-driven pair creation ($\varnothing \to A + B$ at a cost), and structural accumulation. *Key distinction:* structure accumulates irreversibly via the S field; the system does not merely annihilate but builds a frozen record of its interaction history.

Landau theory in non-equilibrium systems. The use of a Landau free energy for bond formation (section 2.9) imports equilibrium phase-transition phenomenology into a far-from-equilibrium, transient context. This is justified because bond formation is a local, fast process relative to the global energy depletion timescale, allowing a quasi-static approximation at the bond level. *Key distinction:* the Landau functional operates in a non-stationary, irreversibly depleting background rather than the stationary or slowly-driven setting of classical non-equilibrium Landau theory.

Summary of distinguishing features. The combination of irreversible finite energy, multi-species asymmetry, Landau bond formation, and regime switching defines a system class that does not reduce to any of the above. Specifically: (i) unlike the contact process, absorption is guaranteed without fine-tuning; (ii) unlike sandpiles, there is no external drive; (iii) unlike $A+B$ annihilation, structure accumulates irreversibly; (iv) unlike equilibrium Landau theory, the phase transition is embedded in a transient, non-stationary context. Table 1 summarises these distinctions systematically.

Table 1: Structural comparison of the present model with related frameworks. A ✓ indicates the feature is present; a dash indicates it is absent or requires fine-tuning.

Feature	Contact Process	Sandpile / SOC	$A+B$ Annihilation	Multi-type IPS	This Model
Multi-species dynamics	–	–	✓	✓	✓
Species asymmetry (forbidden channel)	–	–	–	partial	✓
Finite, non-renewable energy	–	–	–	–	✓
Guaranteed absorption (no tuning)	tuned	–	✓	tuned	✓
Structural memory (S field)	–	–	–	–	✓
Threshold-driven regime switching	–	–	–	–	✓
Landau bond formation	–	–	–	–	✓
Structural hierarchy depth	1	1	1	1–2	4

6.2 Numerical Illustrations

We present three runs that explore qualitatively different regions of the system's initial-condition space. Each illustrates a distinct dynamical regime; together, they show that the model's behaviour is not an artefact of a particular parameter choice.

High-energy dense initial conditions. When $\mathcal{E}_{\text{tot}}(0)$ and the initial excitation densities are both large, the system exhibits a rapid burst of activity, sustained structural growth, and then irreversible decay toward absorption. The dynamics display a characteristic three-phase trajectory: explosive onset, transient complexity peak, and monotone collapse. Figure 3 shows this trajectory. The code is `model_simulation/run_high_energy.py`.

Spatially concentrated initial conditions. Initial energy and excitations are concentrated in the left 25% of the chain; the remainder of the graph starts empty. For this run the interaction rates are reduced and the diffusion constants increased relative to the default values, so that transport and annihilation act on comparable timescales and the propagation front is resolved (at the default rates, annihilation empties the loaded region within a few steps, before diffusion can carry excitations outward). Diffusion and local dynamics then spread activity across the graph until absorption. Figure 4 shows the global time series; Figure 5 shows the spatial distribution at several times, revealing a propagation front that advances outward from the initially active region

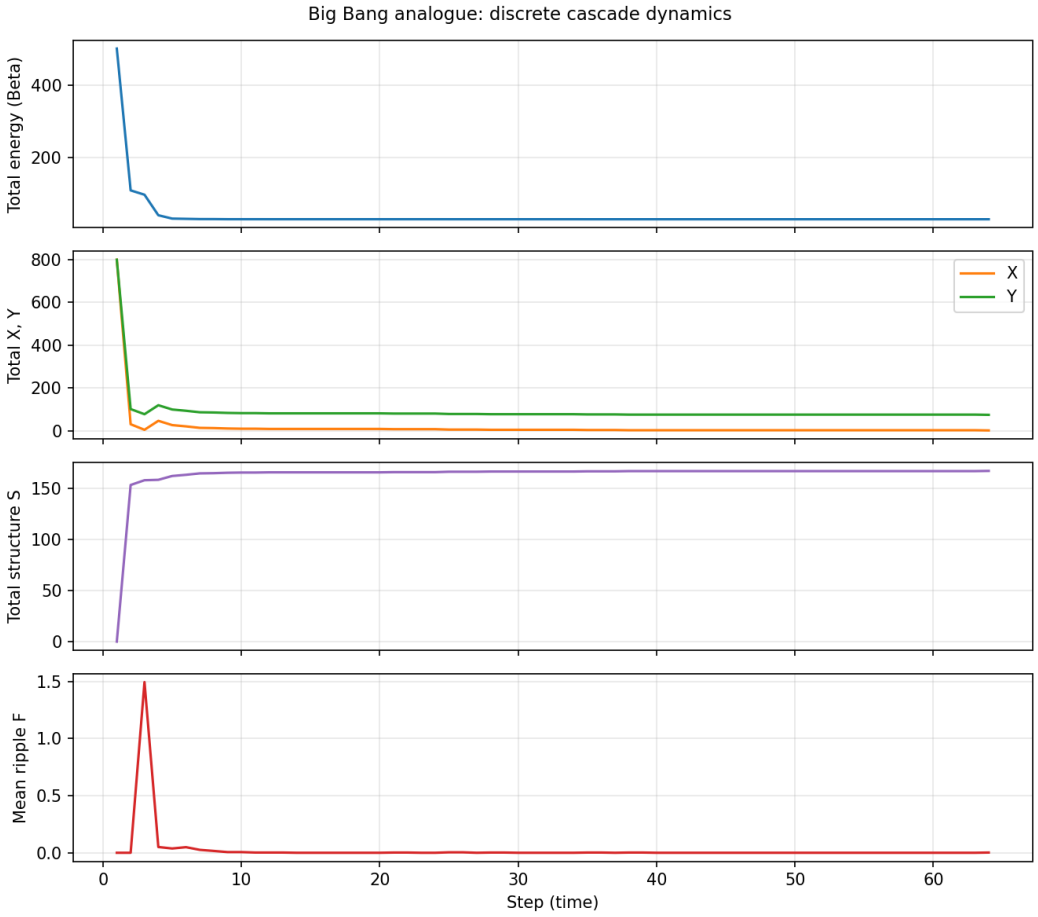

Figure 3: High-energy dense initial conditions ($P = 100$ sites). **Top to bottom:** total energy (monotone decrease, cf. theorem 3.3), total X and Y (asymmetric depletion), total structure S, mean ripple F. The burst-then-decay profile is qualitatively reminiscent of expansion-cooling dynamics.

(the chain is periodic, so the front also wraps around the boundary). The code is `model_simulation/run_spatial_concentration.py`.

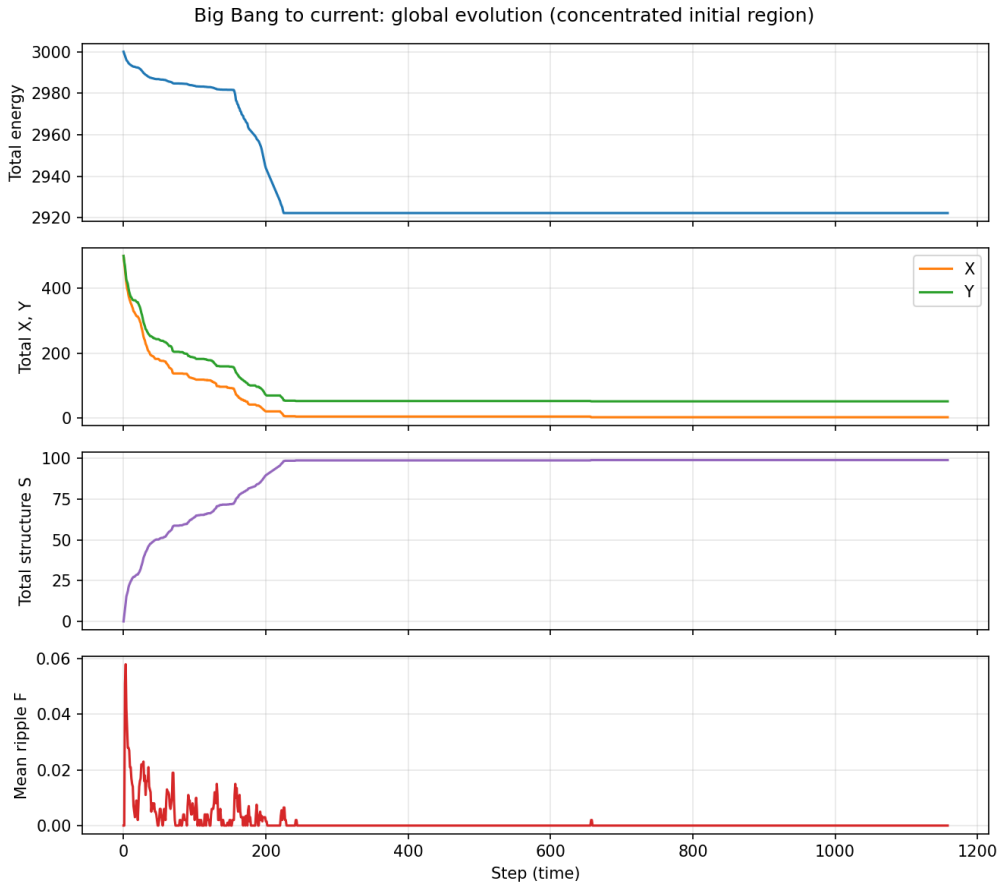

Figure 4: Spatially concentrated initial conditions: global evolution. **Top to bottom:** total energy, total X and Y, total structure S, mean ripple F vs. time. Same run as fig. 5.

Minimal-seed initial conditions. A single small region is given a modest amount of X, Y, and energy; the rest of the graph is empty. Even from this minimal seed, the system triggers the full cascade dynamics: the localised perturbation grows, drives structural accumulation, and eventually decays to absorption (fig. 6). This illustrates that the model admits a minimal-seed regime in which a small initial perturbation suffices to activate the complete dynamical sequence. The code is `model_simulation/run_minimal_seed.py`.

6.3 Open Problems

1. **Universality class.** Does the absorbing-state transition exhibit directed percolation universality, or does the energy constraint define a new universality class?

2. **Cascade size distribution.** What is the distribution of cascade sizes (total excitations created per explosive event)? Preliminary analysis suggests a truncated power law, but rigorous results are lacking.

3. **Structural complexity scaling.** How does the peak structural complexity $\max_n \mathcal{K}(n)$ scale with graph size P and initial energy density ε_0?

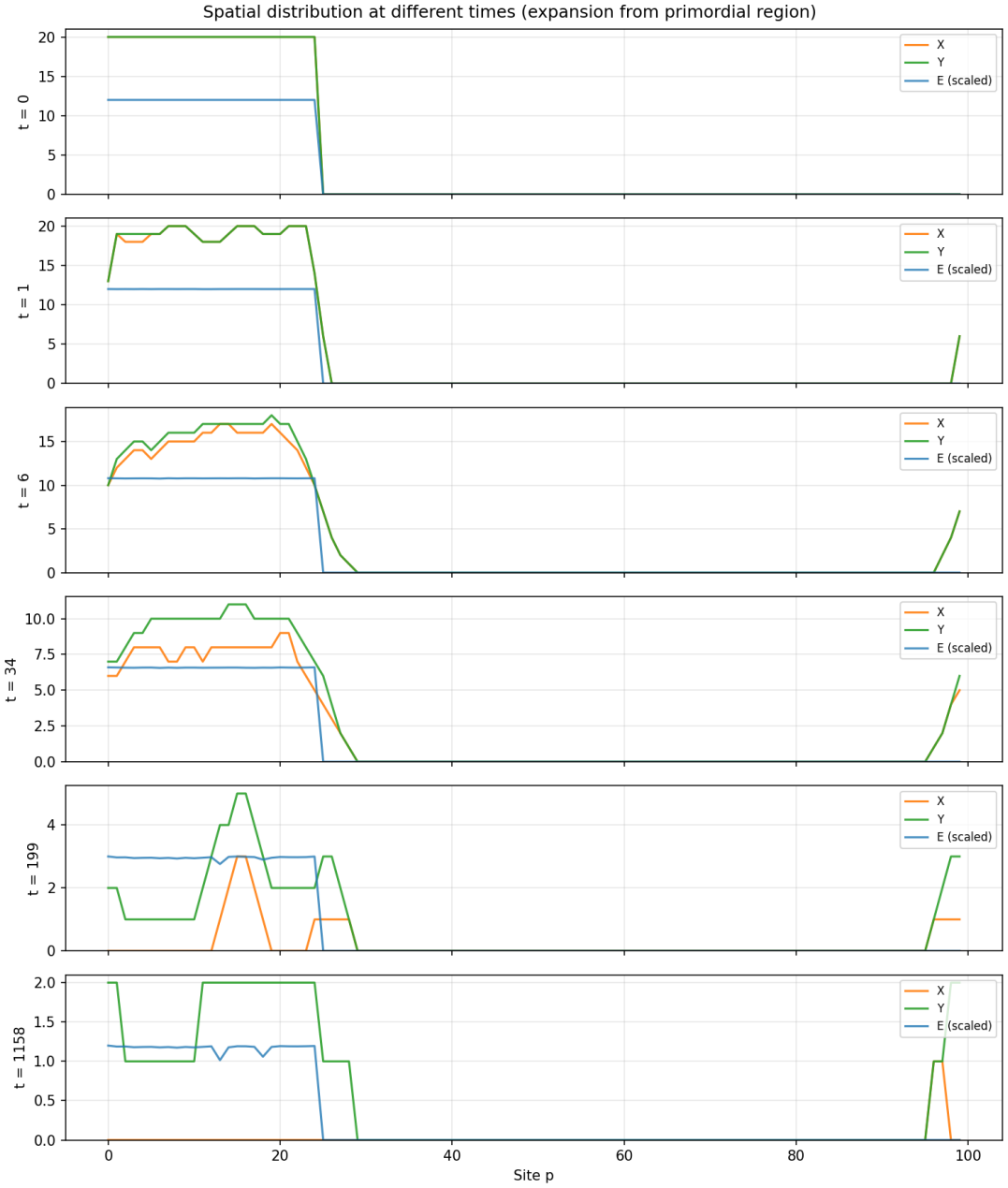

Figure 5: Spatially concentrated initial conditions: spatial distribution of X, Y, and energy (scaled) at several time steps. Activity propagates outward from the initially loaded region until energy depletion halts the dynamics.

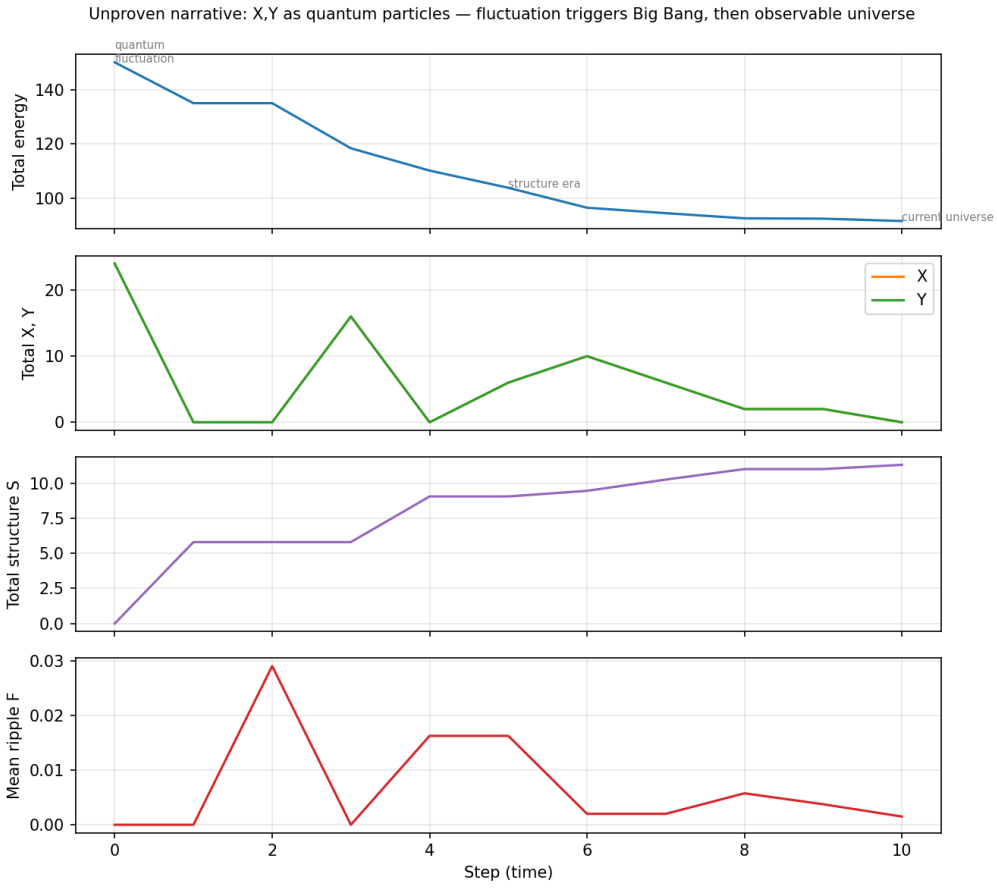

Figure 6: Minimal-seed initial conditions: one small region with X, Y, and energy; rest empty. **Top to bottom:** total energy, total X and Y (asymmetric outcome), total structure S, mean ripple F. The localised perturbation suffices to trigger the cascade.

4. **Infinite-volume limit.** Can the model be extended to $\mathbb{Z}^d$ with appropriate initial conditions? The finite energy constraint may need to be replaced by a density constraint for this limit to be non-trivial.

5. **Continuum limit.** Under appropriate rescaling of space, time, and field variables, does the model converge to a stochastic PDE? Candidates include reaction–diffusion equations with a depleting source term.

6. **Metastable bond lifetimes.** What is the expected lifetime of a bonded configuration before disruption by a nearby explosion? This connects to nucleation theory in statistical mechanics.

7. **Role of asymmetry** (resolved in Part II Goswami [2026b]). What happens in the symmetric limit $\alpha_{XX} = \alpha_{YY}$, $\omega_X = \omega_Y$? Does the structural hierarchy collapse? The forbidden Y–Y channel and the frequency mismatch are constitutive assumptions; understanding their necessity (or relaxation) is an important structural question. *Part II proves that both asymmetries are independently necessary: symmetry causes the hierarchy to collapse, the forbidden Y–Y channel is required for bond formation, and the frequency mismatch, acting through the interference factor* (1)*, is the sole recurrent deterministic drive of the ripple, with explicit beat amplitude and an explicit critical frequency asymmetry.*

6.4 Limits and Scope

We state explicitly what this model does *not* claim and where its guarantees break down.

No continuum claim. The model is defined entirely on a finite graph with discrete state variables and discrete time. We make no claim that it converges to a continuum PDE or field theory under rescaling; whether a meaningful continuum limit exists is an open problem (section 6, Open Problem 5).

No physical identification. The simulations in section 6 exhibit dynamics qualitatively reminiscent of expansion-cooling and fluctuation-triggered cascades. These are *observations about the dynamical system*, not claims of physical equivalence to cosmological or quantum processes. The model is a mathematical object; any physical interpretation would require independent justification.

Finite graphs only. All results assume a finite graph $\mathcal{G} = (\mathcal{V}, \mathcal{E})$ with $|\mathcal{V}| < \infty$. This is not merely a technical convenience: finiteness of the graph *combined* with finiteness of the energy is what drives the central guarantees. A finite graph has finitely many vertices, each carrying non-negative energy that decreases strictly under activity; the total energy $\mathcal{E}_{\text{tot}} = \sum_p \mathcal{E}(p)$ is therefore a non-negative supermartingale on a finite state space, which must converge. On an infinite lattice with infinite total energy, this argument fails, and absorption is no longer guaranteed without additional assumptions (Open Problem 4).

Landau functional as decision rule. The Landau free-energy governs bond formation as a static threshold criterion (theorem 2.15), not as a dynamical equation. We do not claim that the Landau functional describes the *time evolution* of the order parameter; it determines only *whether* a bond forms at a given step.

Phase diagram is qualitative. The phase diagram (section 4) identifies the principal dynamical regimes and their boundaries in terms of initial energy density and interaction strength. The boundaries are derived from scaling arguments and simulation; they are not sharp critical surfaces in the sense of equilibrium statistical mechanics.

Simulation is illustrative, not evidential. The numerical results in section 6 illustrate the dynamical regimes but play no role in the proofs, which are self-contained. No theorem in this paper depends on simulation output. The simulations serve a complementary purpose: they make the system's behaviour space visible across different initial conditions and graph topologies, allowing the reader to build intuition for the dynamics that the theorems guarantee.

6.5 Limiting Cases and Reductions

The model contains several classical systems as limiting cases, providing formal anchoring within the existing literature.

Symmetric limit $\to$ single-species annihilation. When $\alpha_{XX} = \alpha_{YY}$ and $\omega_X = \omega_Y$ (so that the interference factor is identically 1), the two-species system degenerates into an effective single-species annihilation–diffusion process on the total excitation count $Z = X + Y$; the reduction is exact (equality in law for Z) in the fully symmetric case $\alpha_{XY} = \alpha_{XX} = \alpha_{YY}$. This is precisely the $A + A \to \varnothing$ system studied in Toussaint & Wilczek [1983], restricted to a finite graph with a finite energy budget. Part II Goswami [2026b] formalises this reduction and proves that the Landau bond-formation mechanism becomes inoperative.

Infinite-energy limit $\to$ multi-type IPS. If we formally set $\mathcal{E}_{\text{tot}}(0) = \infty$ (or remove the energy constraint), the system becomes a multi-type interacting particle system with species-dependent annihilation and diffusion on a finite graph. The energy monotonicity and finite activity theorems no longer hold; absorption is no longer guaranteed, and the system may exhibit an active steady state, analogous to the behaviour of the multi-type contact process [Neuhauser, 1992].

No self-interaction $\to$ pure $A + B$ annihilation. Setting $\alpha_{XX} = \alpha_{YY} = 0$ (no self-interactions) reduces the interaction dynamics to pure two-species annihilation $A + B \to \varnothing$ with energy costs. The energy constraint still enforces guaranteed absorption, but the depletion asymmetry vanishes and the bond-formation mechanism weakens (no minority-species concentration).

These reductions show that the present model occupies a specific point in a broader parameter space: it is the finite-energy, asymmetric-species extension of classical annihilation–diffusion dynamics, with the Landau bond mechanism activated only when both the energy constraint and the species asymmetry are present.

6.6 Potential Extensions

- **Multiple excitation species.** Generalise from two species to K species with species-specific interaction rules and energy costs.
- **Adaptive graph topology.** Allow the graph $\mathcal{G}$ itself to evolve, adding edges where bonds form, removing edges where energy is depleted.
- **External driving.** Add a slow energy injection term to study the transition from guaranteed absorption to possible steady-state behaviour (connecting to SOC models).
- **Spatial energy transport.** Allow $\mathcal{E}$ to diffuse, creating energy gradients and directed flows.

7 Conclusion

We have introduced a discrete stochastic cascade model on finite graphs that couples four state variables (two excitation species, a capacity energy field, and a structural state) through layered update rules with three dynamical regimes. The model is fully specified by the twenty parameters listed in section 2.3 and a choice of graph topology.

The central structural result is that the total capacity energy is a strict Lyapunov function (non-negative supermartingale) for the dynamics: it decreases at every active time step and cannot increase. This single invariant implies finite total activity, almost sure absorption, and a strict thermodynamic arrow, all as rigorous consequences, not assumptions.

The model generates rich transient phenomena. In the cascade regime, explosive pair creation amplifies activity in self-limiting bursts, building spatially heterogeneous structural configurations before the system freezes into a unique, history-dependent absorbing state. Bond formation is governed by a Landau free-energy functional that embeds a local order–disorder phase transition within the global irreversible dynamics.

The framework provides a minimal, internally consistent setting for studying the interplay between stochastic interactions, irreversible resource depletion, threshold-driven instabilities, and emergent structure. It sits at the intersection of interacting particle systems, absorbing-state phase transitions, and reaction–diffusion dynamics, and raises several open questions regarding universality, scaling, and continuum limits that merit further investigation.

Outlook. More broadly, the results suggest that discrete asymmetry combined with irreversible resource constraints may be a general mechanism for producing transient structural complexity in stochastic systems. Whether analogous hierarchy-forming dynamics arise in other settings where non-interchangeable agents consume a shared finite resource (e.g., ecological competition, distributed computing with finite energy budgets, or catalytic chemistry with irreversible substrate depletion) is an open and, we believe, fertile direction. The model's reduction to known systems in limiting cases (section 6) provides a concrete anchor for such extensions.

A Simulation Pseudocode

The update rule is split across algorithms 1 and 2 so that each float fits on one page: algorithm 1 performs all stochastic and deterministic operations at a single vertex at time n; algorithm 2 wraps the global time step (local sweeps, diffusion, termination).

B Parameter Sensitivity

The qualitative behaviour is controlled by a small number of dimensionless ratios:

Ratio	Controls	Effect of increasing
$\alpha_{XY}\omega_X\omega_Y\,\rho_0/C$	Cascade onset	Easier to trigger explosions
α_{XX}/α_{XY}	Self- vs. cross-interaction	More X depletion, fewer bonds
ω_X/ω_Y	Frequency asymmetry	Stronger species differentiation
$\mathcal{E}_{\text{tot}}(0)/(k_{XY}\,P\,\rho_0)$	System lifetime	Longer active phase
η/k_{XY}	Explosion cost ratio	Fewer but costlier explosions
$D_X\ \deg_{\max}$	Diffusion strength	Faster spatial mixing
T_c	Bond formation ease	More bonds at higher T_c
κ/k_{XY}	Bond vs. interaction cost	Relative bond preference

C Key Equations Summary

For quick reference, the main equations of the model are collected below.

- **Interaction rates:** $R_{XY} = \alpha_{XY}\,\omega_X\,\omega_Y\,\Theta(n)\,X\,Y$ with interference factor $\Theta(n) = \vartheta + (1-\vartheta)[1+\cos((\omega_X-\omega_Y)n)]/2$, $R_{XX} = \alpha_{XX}\,\omega_X^2\,X(X-1)/2$; Y–Y is forbidden ($\alpha_{YY}=0$).
- **Ripple:** $F(p,n) = |S(p,n) - 2\,S(p,n{-}1) + S(p,n{-}2)| = |\Delta^2 S(p,n)|$.
- **Leakage:** $L = \lambda\,F$ when $C < F < C+\Delta$.
- **Explosion:** $m = \lfloor (F-C)/\Delta \rfloor$, $M = \eta\,m$ when $F \geq C+\Delta$.
- **Energy update:** $\mathcal{E}(p,n{+}1) = \mathcal{E}(p,n) - k_{XY}N_{XY} - k_{XX}N_{XX} - L - M - \kappa B$, clamped to ≥ 0.
- **Structural update:** $S(p,n{+}1) = S(p,n) + \gamma_1\,N_{XY} + \gamma_{XX}\,N_{XX} + \gamma_2\,B$.
- **Global invariant:** $\mathcal{E}_{\text{tot}}(n{+}1) = \mathcal{E}_{\text{tot}}(n) - \mathcal{D}(n)$, $\mathcal{D}(n) \geq 0$; strict decrease when active.

References

P. Bak, C. Tang, and K. Wiesenfeld. Self-organized criticality: An explanation of the $1/f$ noise. *Physical Review Letters*, 59(4):381–384, 1987.

H. Berestycki, L. Nirenberg, and V. Volpert. Reaction-diffusion equations for population dynamics with spatial constraints. *Journal of Mathematical Physics*, 50(1):013505, 2009.

L. Bertini, A. De Sole, D. Gabrielli, G. Jona-Lasinio, and C. Landim. Macroscopic fluctuation theory. *Reviews of Modern Physics*, 87(2):593, 2015.

L. Böttcher, O. Woolley-Meza, N. A. M. Araújo, H. J. Herrmann, and D. Helbing. Disease-induced resource constraints can trigger explosive epidemics. *Nature Communications*, 6(1):1–7, 2015.

M. Bramson and J. L. Lebowitz. Asymptotic behavior of densities in diffusion-dominated annihilation reactions. *Physical Review Letters*, 61(21):2397–2400, 1988.

J. L. Cardy. Renormalisation group approach to reaction-diffusion problems. *Field Theory and Statistical Mechanics*, 1999.

B. Chopard and M. Droz. *Cellular Automata Modeling of Physical Systems*. Cambridge University Press, 1998.

M. C. Cross and P. C. Hohenberg. Pattern formation outside of equilibrium. *Reviews of Modern Physics*, 65(3):851–1112, 1993.

D. Dhar. Self-organized critical state of sandpile automaton models. *Physical Review Letters*, 64(14):1613–1616, 1990.

R. Durrett and S. Levin. The importance of being discrete (and spatial). *Theoretical Population Biology*, 46(3):363–394, 1994.

T. Galla. Multi-species trait-dependent demographic evolution in spatial models. *Journal of Statistical Mechanics: Theory and Experiment*, 2011(08):P08007, 2011.

S. Goswami. Discrete stochastic cascade dynamics on finite graphs with irreversible energy depletion. Part II: Necessity of species asymmetry for structural hierarchy. *Submitted*, 2026.

G. R. Grimmett. Interacting Particle Systems. *Interacting Particle Systems*, Springer, 1999.

T. E. Harris. Contact interactions on a lattice. *The Annals of Probability*, 2(6):969–988, 1974.

M. Henkel, H. Hinrichsen, and S. Lübeck. *Non-Equilibrium Phase Transitions, Volume 1: Absorbing Phase Transitions*. Springer, 2008.

H. Hinrichsen. Non-equilibrium critical phenomena and phase transitions into absorbing states. *Advances in Physics*, 49(7):815–958, 2000.

P. C. Hohenberg and B. I. Halperin. Theory of dynamic critical phenomena. *Reviews of Modern Physics*, 49(3):435–479, 1977.

H. K. Janssen. On the nonequilibrium phase transition in reaction-diffusion systems with an absorbing stationary state. *Zeitschrift für Physik B Condensed Matter*, 42(2):151–154, 1981.

P. L. Krapivsky, S. Redner, and E. Ben-Naim. *A Kinetic View of Statistical Physics*. Cambridge University Press, 2010.

L. D. Landau. On the theory of phase transitions. *Zh. Eksp. Teor. Fiz.*, 7:19–32, 1937. [Reprinted in *Collected Papers of L.D. Landau*, Pergamon, 1965].

B. P. Lee. Renormalization group calculation for the reaction $kA \to \varnothing$. *Journal of Physics A*, 27(8):2633–2652, 1994.

T. M. Liggett. *Stochastic Interacting Systems: Contact, Voter and Exclusion Processes*. Springer, 1999.

K. Mallick. The exclusion process: A paradigm for non-equilibrium behaviour. *Physica A: Statistical Mechanics and its Applications*, 418:17–48, 2015.

J. Marro and R. Dickman. *Nonequilibrium Phase Transitions in Lattice Models*. Cambridge University Press, 1999.

M. A. Muñoz. Colloquium: Criticality and dynamical scaling in living systems. *Reviews of Modern Physics*, 90(3):031001, 2018.

C. Neuhauser. Ergodic theorems for the multitype contact process. *Probability Theory and Related Fields*, 91(3–4):467–506, 1992.

G. Ódor. Universality classes in nonequilibrium lattice systems. *Reviews of Modern Physics*, 76(3):663–724, 2004.

R. Pastor-Satorras, C. Castellano, P. Van Mieghem, and A. Vespignani. Epidemic processes in complex networks. *Reviews of Modern Physics*, 87(3):925, 2015.

L. Peliti. Path integral approach to birth-death processes on a lattice. *Journal de Physique*, 46(9):1469–1483, 1985.

V. Privman. *Nonequilibrium Statistical Mechanics in One Dimension*. Cambridge University Press, 1997.

U. Seifert. Stochastic thermodynamics, fluctuation theorems and molecular machines. *Reports on Progress in Physics*, 75(12):126001, 2012.

U. C. Täuber. *Critical Dynamics: A Field Theory Approach to Equilibrium and Non-Equilibrium Scaling Behavior*. Cambridge University Press, 2014.

U. C. Täuber. Phase transitions and scaling in systems far from equilibrium. *Annual Review of Condensed Matter Physics*, 8:185–210, 2017.

D. Toussaint and F. Wilczek. Particle–antiparticle annihilation in diffusive motion. *The Journal of Chemical Physics*, 78(5):2642–2647, 1983.

N. G. Van Kampen. *Stochastic Processes in Physics and Chemistry*. Elsevier, 1992.

Algorithm 1 Local vertex update LocalVertex(p, n). $\mathcal{E}(p)$ denotes capacity energy. X–X self-interaction is computed; Y–Y is absent.

Cross-interaction (X–Y), phase-modulated
$\Theta \leftarrow \vartheta + (1-\vartheta)\big[1+\cos\big((\omega_X-\omega_Y)\,n\big)\big]/2$
$R_{XY} \leftarrow \alpha_{XY}\,\omega_X\,\omega_Y\,\Theta\,X(p)\,Y(p)$
$N_{XY} \leftarrow \min\big(\mathrm{Poi}(R_{XY}),\ X(p),\ Y(p)\big)$
$X(p) \leftarrow X(p) - N_{XY}$; $Y(p) \leftarrow Y(p) - N_{XY}$
Self-interaction (X–X); Y–Y forbidden
$R_{XX} \leftarrow \alpha_{XX}\,\omega_X^2\,X(p)\big(X(p)-1\big)/2$
$N_{XX} \leftarrow \min\big(\mathrm{Poi}(R_{XX}),\ \lfloor X(p)/2 \rfloor\big)$
$X(p) \leftarrow X(p) - 2\,N_{XX}$
Ripple
if $n \geq 2$ **then**
    $F \leftarrow \big|S(p,n) - 2\,S(p,n-1) + S(p,n-2)\big|$
else
    $F \leftarrow 0$
end if
Regime classification and explosion
$L \leftarrow 0$; $M \leftarrow 0$; $m \leftarrow 0$
if $C < F < C + \Delta$ **then**
    $L \leftarrow \lambda\,F$
else if $F \geq C + \Delta$ **then**
    $L \leftarrow \lambda\,F$
    $m \leftarrow \lfloor (F - C)/\Delta \rfloor$; $M \leftarrow \eta\,m$
    if $M > \mathcal{E}(p)$ **then**
        $m \leftarrow \lfloor \mathcal{E}(p)/\eta \rfloor$; $M \leftarrow \eta\,m$
    end if
    $X(p) \leftarrow X(p) + m$; $Y(p) \leftarrow Y(p) + m$
end if
Bond formation (Landau free energy)
$\psi \leftarrow \sqrt{X(p)\cdot Y(p)}$; $T_{\mathrm{eff}} \leftarrow F/C$
$\partial\mathcal{F}/\partial\psi \leftarrow 2\,a_0(T_{\mathrm{eff}} - T_c)\,\psi + 4b\,\psi^3$
$B \leftarrow 0$
if $\partial\mathcal{F}/\partial\psi < 0$ **and** $\psi > 0$ **then**
    $B \leftarrow \min\big(\lfloor \psi^2 |\partial\mathcal{F}/\partial\psi| / b \rfloor,\ \lfloor \mathcal{E}(p)/\kappa \rfloor,\ X(p),\ Y(p)\big)$
    $X(p) \leftarrow X(p) - B$; $Y(p) \leftarrow Y(p) - B$
end if
Energy and structural updates
$cost \leftarrow k_{XY}\,N_{XY} + k_{XX}\,N_{XX} + L + M + \kappa\,B$
$\mathcal{E}(p) \leftarrow \max\big(\mathcal{E}(p) - cost,\ 0\big)$
$S(p) \leftarrow S(p) + \gamma_1\,N_{XY} + \gamma_{XX}\,N_{XX} + \gamma_2\,B$
if $N_{XY} + N_{XX} + L + M + B > 0$ **then**
    $active \leftarrow$ TRUE
end if

Algorithm 2 Main simulation loop (calls algorithm 1 at each vertex each time step).

Require: Graph $\mathcal{G} = (\mathcal{V}, \mathcal{A})$, parameters, initial fields $X(p)$, $Y(p)$, $\mathcal{E}(p)$, $S(p)$ for all $p \in \mathcal{V}$

for $n = 0, 1, 2, \ldots$ **do**
    $active \leftarrow$ FALSE

    for each vertex $p \in \mathcal{V}$ **do** ▷ Local updates
        LOCALVERTEX(p,n)
    end for

    Diffusion (conservative; energy does not diffuse)
    for each vertex $p \in \mathcal{V}$ **do**
        $X(p) \leftarrow X(p) + D_X \sum_{q \in \mathcal{N}(p)} [X(q) - X(p)]$
        $Y(p) \leftarrow Y(p) + D_Y \sum_{q \in \mathcal{N}(p)} [Y(q) - Y(p)]$
    end for
    Round all $X(p)$, $Y(p)$ to nearest non-negative integer
    if $\neg\, active$ **then**
        break ▷ Absorbing state reached
    end if
end for